論文99-36D-4-5

SAR Imaging에서 Physical Array와 합성 Array 신호의 Subspace 비교를 통한 Wavefront Inversion 기법 입증

(Verification of Wavefront Inversion Scheme via Signal Subspace Comparison Between Physical and Synthesized Array Data in SAR Imaging)

崔 貞 姬 *

(Jeong-Hee Choi)

요 약

Synthetic Aperture Radar 시스템은 레이더 또는 목적물을 일정거리 또는 시간 간격동안 움직여가면서 반사되는 신호를 측정하여 동시에 처리해 줌으로써 안테나 크기를 크게 하는 효과를 가지게 되므로 목적물의 형체를 파악하는 Imaging 시스템의 일종이다. Imaging의 성패는 어떤 Modeling과 Inversion 과정을 거치느냐에 달려 있는데 본 논문에서는 가장 Approximation이 적은 Wavefront reconstruction 기법을 적용하여 SAR 모델에서 획득한 데이터와 같은 크기의 실제 안테나가 있다고 가정하였을 때의 데이터와 이론적이고 실험적인 Signal Subspace 비교를 수행하였다. 이 연구를 통해 새로운 기법인 Wavefront reconstruction 알고리즘을 충분히 뒷받침해 줄 수 있는 결과를 얻을 수 있다.

Abstract

Unlike the traditional radar system, Synthetic Aperture Radar(SAR) system is capable of imaging a target scene to certain degree of cross-range resolution. And this resolution is mainly depends on the size of aperture synthesized. Thus, a good system model and inversion scheme should be developed to actually give effect of synthesizing aperture size, which in turn gives better cross range resolution of reconstructed target scene. Among several inversion schemes for SAR imaging, we used an inversion scheme called wavefront reconstruction which has no approximation in wave propagation analysis, and tried to verify whether the collected data with synthesized aperture actually give the same support as that with physical aperture in the same size. To do this, we performed a signal subspace comparison of two imaging models with physical and synthesized arrays, respectively. Theoretical comparisons and numerical analysis using Gram-Schmidt procedures have been performed. The results showed that the synthesized array data fully span the physical array data with the same system geometry. This result strongly supports the previously proposed inversion scheme valuable in high resolution radar imaging.

* 正會員, 大邱大學校 情報通信工部

(Dept. of Computer and Communication, Taegu Univ.)

※ 본 논문은 1998년 정보통신부의 대학기초연구지원 사업으로 일부 수행됨.

接受日字:1999年1月29日, 수정완료일:1999年3月24日

I. Introduction

With the traditional radar system, we can only estimate the ditance between target scene and radar, and decide whether the target exist or not.

It is because of the limitation of radar antenna size compared with distance between the radar and the target. Unlike the traditional radar system, a new radar technology called Synthetic Aperture Radar (SAR) is capable of imaging a target as well as ranging and detection of the target. This imaging radar system employs synthesizing aperture techniques instead of using huge size physical antennas by moving radar(SAR) or target(Inverse SAR) in echo data collection. Thus, a good system model and inversion scheme should be developed to actually give effect of synthesizing aperture size, which in turn gives better cross range resolution of reconstructed target scene.

In this paper, we make a comparison of two imaging models which have physical and synthesized arrays, to verify the wavefront inversion scheme actually gives aperture synthesizing effect. Both of them have the same system geometry except that one uses physical fixed array as an aperture while the other synthesizes the same size of aperture through the Doppler processing.

The inversion based on each model is a computationally manageable method that incorporates the radiation pattern of each element on the array at the transmit and receive modes. For this comparison, we use the wavefront inversion equation of synthetic aperture radar imaging [4] and that of physical aperture discussed in detail in this paper.

This study indicates that a physical array and its synthesized counterpart possess the same *resolution* despite of the fact that the synthesized array's signal subspace is a subset of much larger signal subspace for the physical array. This study also shows that the data from physical array contains redundant information as compared with the synthesized counterpart. Therefore, it turns out that these results strongly support the wavefront inversion scheme for SAR Imaging.

Such echo imaging techniques applies to raw data processing of various remote sensing problems such as geophysical exploration, environmental monitoring, and reconnaissance for military purposes [1] [2] [3].

II. System model and inversion

We consider the system model and the inversion for a monostatic and ground-plane physical and synthesized array with a source of spherical radiation pattern(See Fig. 1). The (x, y) coordinate represents range and cross range, respectively. The wave traveling in the medium surrounding the target has temporal frequency of ω and the source signal has certain bandwidth centered at carrier frequency.

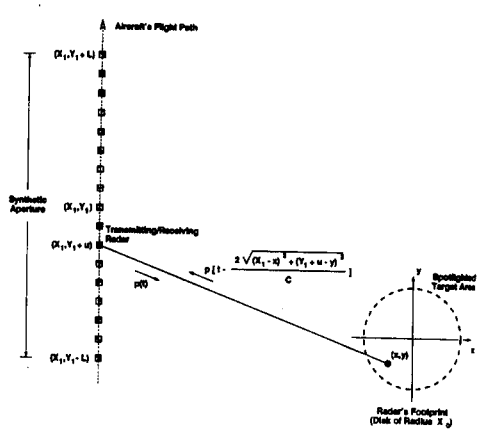

그림 1. Monostatic SAR 시스템의 기하학적 배치
Fig. 1. Monostatic SAR imaging system geometry.

1. Physical array

A physical array is a group of Single Element Transducers (SETs) fixed on the line and all SETs record returning signal from the object area at the same time for the one source of SETs. The system geometry is the same as that of the SAR system except that a group of SETs are fixed along the line $x = X_1$ in the (x, y) plane instead of moving a SET along the line.

This physical array makes a transmission at (X_1, Y_1+u) and its corresponding reception at all SETs (X_1, Y_1+v) for $u \in [-L, +L]$, $v \in [-L, +L]$ on the (x, y) plane. Since the radar's radiation pattern at far field is spherical, the phase delays by a point scatterer at (x, y) for the transmit-mode and receive-mode are

$k\sqrt{(X_1-x)^2+(Y_1+u-y)^2}$ and

$k\sqrt{(X_1-x)^2+(Y_1+v-y)^2}$, respectively,

when we assume to have huge size of physical array antenna. Thus, the total recorded echoed signal from the target area at physical array is

$$p(u, v, \omega) = \int\int f(x, y)\exp[jk\sqrt{(X_1-x)^2+(Y_1+u-y)^2}] \cdot \exp[jk\sqrt{(X_1-x)^2+(Y_1+v-y)^2}]dx\,dy \quad (1)$$

, where $f(x, y)$ is the object's reflectivity function.

The spherical wave with wavenumber k, i.e., $\exp[jk\sqrt{(X_1-x)^2+(Y_1+u-y)^2}]$, has spectral decomposition of the SET's radiation pattern as follows :

$$\int_{-\infty}^{\infty} \frac{\exp[j(\sqrt{k^2-k_u^2}(X_1-x)+k_u(Y_1+u-y)]}{\sqrt{k^2-k_u^2}}\,dk_u \quad (2)$$

, where k_u represents the *Fourier* transform pair of u.

Similarly for v, we have

$$\int_{-\infty}^{\infty} \frac{\exp[j(\sqrt{k^2-k_v^2}(X_1-x)+k_v(Y_1+v-y)]}{\sqrt{k^2-k_v^2}}\,dk_v \quad (3)$$

, where k_v represents the *Fourier* transform pair of v.

By substituting (2) and (3) into (1) and after some rearrangements (amplitude suppressed), one obtains

$$p(u, v, \omega) = \int_{-\infty}^{\infty} dk_u \int_{-\infty}^{\infty} dk_v F(\sqrt{k^2-k_u^2}+\sqrt{k^2-k_v^2}, k_u+k_v) \cdot \exp[j(\sqrt{k^2-k_u^2}+\sqrt{k^2-k_v^2})X_1]\ \exp[j(k_u u+k_v v)] \quad (4)$$

Note that $F(*,*)$ is *Fourier* counterpart of $f(x, y)$.

Taking the spatial Fourier transform of both sides of (4) with respect to u and v yields,

$$P(k_u, k_v, \omega) = F(\sqrt{k^2-k_u^2}+\sqrt{k^2-k_v^2},\ k_u+k_v) \cdot \exp[j(\sqrt{k^2-k_u^2}+\sqrt{k^2-k_v^2})X_1 + j(k_u+k_v)Y_1] \quad (5)$$

Finally, from (5) we can write the following inversion equation:

$$F(k_x, k_y) = \exp[-jk_x X_1 - jk_y Y_1]P(k_u, k_v, \omega),$$

, where $k_x \equiv \sqrt{k^2-k_u^2}+\sqrt{k^2-k_t^2}$ and

$$k_y \equiv k_u + k_t \quad (6)$$

Therefore, the echoed data at physical array in the spatial and temporal frequency domain are mapped into the spatial frequency domain of the target via (6). (See Fig. 2)

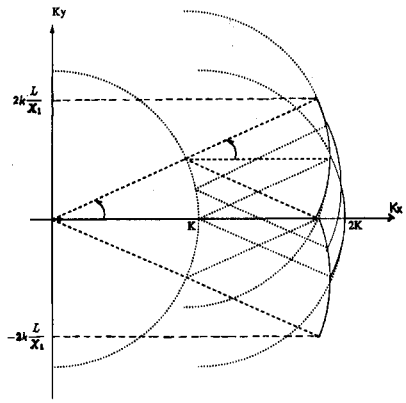

그림 2. Target의 Spatial Frequency 영역에서의 Physical array 데이터 분포

Fig. 2. Coverage of Physical array data in spatial frequency domain of target.

2. Synthesized array

In the SAR imaging system, the echoed data are collected by moving radar's position with respect to the target area. Now assume that a

monostatic radar is mounted on a vehicle such as an aircraft or satellite moving along certain prescribed path instead of having huge size of physical array antenna. At each position of u, radar transmit source signal and collect echoed signal while it is moving along the path [4]. In this paper, we simply assume the path is linear where the transmission and reception occurs at $[X_1, Y_1+u]$ for $u\in[-L, +L]$.

With the same system geometry as physical array, the phase delay for Synthetic Aperture Radar is $2k\sqrt{(X_1-x)^2+(Y_1+u-y)^2}$ and the total recorded data from the point target located at (x, y) is represented as

$$s(u,\omega) = \int\int f(x,y)\exp[j\,2k\sqrt{(X_1-x)^2+(Y_1+u-y)^2}]dxdy \tag{7}$$

The inversion equation is

$$F(k_x, k_y) = \exp[-jk_xX_1 - jk_yY_1]S(k_u, \omega)$$

, where $k_x \equiv \sqrt{4k^2-k_u^2}$ and

$$k_y \equiv k_u \tag{8}$$

From (8), the coverage of the temporal and spatial frequency domain data in the spatial frequency domain of target, i.e., $F(k_x, k_y)$, is depicted as Fig. 3.

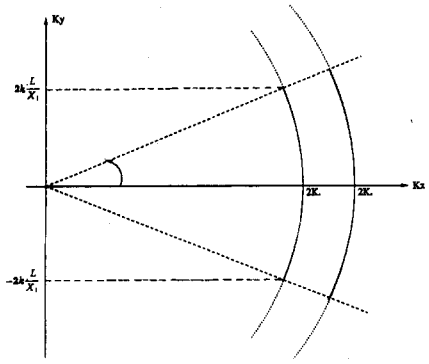

그림 3. Target의 Spatial Frequency 영역에서의 Synthesized array 데이터 분포.
Fig. 3. Coverage of SAR data in the spatial frequency domain of target.

Ⅲ. Signal subspace comparison

1. Theoretical Study

Recall that $s(u,\omega)$ is the recorded data at the synthesized aperture. If there are N unique measurements made for a synthesized array, the number of unique data for a physical array is $\frac{N(N+1)}{2}$. Moreover, the signal subspace of the synthesized array data is a subset of the signal subspace for the physical array of the same size. Despite of this fact, the following clues raise the question of whether a physical array data contain redundant information or not.

- *Fact 1* : Fig. 2. and Fig. 3. based on the facts in (6) and (8) indicate that the spatial frequency coverage obtained via a physical array and a synthesized array of the same size are approximately identical.

- *Fact 2* : From the results in [4], it can be shown that the cross-range resolution in the broadside case for both the physical and synthesized array is $\Delta y = \frac{X_1\lambda}{4L}$, where $\lambda = \frac{2\pi}{k}$ is the wavelength of the impinging field and L is half of the aperture size.

- *Fact 3* : The empirical studies show that the physical arrays yield images with cross-range resolutions that are slightly inferior to those of synthesized arrays of the same size. This can be attributed to the fact that the two-dimensional discrete Fourier transforms performed in the (u, v) domain for a physical array produces more numerical errors than the one-dimensional discrete *Fourier* transform in u domain for a synthesized array.

In addition to the above Fact 1, 2 and 3, we can prove that physical array data for a point scatterer can be represented via a linear combination of the synthetic aperture data for the

point scatterer.

If we consider only one point target in the object region, that is, $f(x,y)=\delta(x-x_0, y-y_0)$, then the recorded signals using physical and synthesized arrays are

$$p(u,v,\omega) = \exp[jk\sqrt{(X_1-x_0)^2+(u-y_0)^2}]\cdot \exp[jk\sqrt{(X_1-x_0)^2+(v-y_0)^2}] \quad (9)$$

and

$$s(u,\omega)=\exp[j2k\sqrt{(X_1-x_0)^2+(u-y_0)^2}] \quad (10)$$

For notational simplicity, we consider the case of $Y_1=0$, i.e., broad side case.

What we want is to compare these data in temporal and spatial frequency domain. Thus, by taking the *Fourier* transform of (9) and (10) in both (u,v) domain and spatially shifting this data into object region by multiplying $\exp[-jk_xX_1-jk_yY_1]$ with an approximation of $X_1 \gg x_0$ according to the relationship in (6) and (8). We then obtain

$$P(k_u,k_v,\omega) \simeq A(k_u,k_v)\exp[-j(k_u+k_v)y_0] \quad (11)$$

and

$$S(k_u,\omega) \simeq B(k_u)\exp[-j k_u y_0] \quad (12)$$

, where $A(k_u,k_v)=\frac{1}{\sqrt{k^2-k_u^2}\sqrt{k^2-k_v^2}}$

and $B(k_u)=\frac{1}{\sqrt{4k^2-k_u^2}}$

Note that either $A(k_u,k_v)$ or $B(k_u)$ is an amplitude function. From (11) and (12), we can represent $P(k_u,k_v,\omega)$ in terms of $S(k_u,\omega)$ for a fixed k_v.

That is

$$P(k_u,k_v,\omega)\simeq C(k_u,k_v)S(k_u,\omega) \quad (13)$$

, where

$$C(k_u,k_v)=\frac{A(k_u,k_v)\exp(-jk_yy_0)}{B(k_u)}$$

The total frequency coverage of the echoed data in (k_x,k_y) domain, consists of frequency coverage from each point target. In other words, the signal subspace of the Fourier domain data by one point target is a subset of the one by all point targets in the object region. Therefore, comparison of signal subspaces of physical and synthesized array data from one point target, gives the same conclusion in dealing with the total echoed signal subspace from the object area to be imaged. We also proved this relationship numerically next.

2. Numerical Study Using Gram-Schmidt Procedures

If an arbitrary vector $\bar{e}$ is in a signal subspace completely spanned by a set of orthonormal basis vectors, $\bar{\phi}_i$, where $i=1,..M$, then $\bar{e}$ can be completely represented by a linear combination of $\bar{\Phi}_i$'s.

That is

$$\bar{e} = \sum_{i=1}^{M}\langle \bar{e},\bar{\phi}_i\rangle \bar{\phi}_i \quad (14)$$

, where $\langle\cdot,\cdot\rangle$ represents the inner product of two vectors.

In the same manner, if each vector in the signal subspace of the physical array data , *i.e.*, $P(k_u,k_v,\omega)$, can be represented by a linear combination of orthonormal basis vectors, *i.e.*, $\bar{\phi}_i$'s, induced from the synthesized array data, *i.e.*, $S(k_u,\omega)$, then the size of the signal subspace from physical array data is the same as that from synthesized counterpart.

We use the Gram-Schmidt procedure to construct an orthonormal set of basis functions from the discrete two-dimensional synthetic aperture data, *i.e.*, $S(k_u,\omega)$. We then project the discrete three-dimensional physical array data, i.e., $P(k_u,k_v,\omega)$ onto the signal subspace spanned by the orthonormal basis functions (or, equivalently, the synthetic aperture data). We

then compare the obtained signal, i.e.,

$$\hat{P}(k_u, k_v, \omega) = \sum_{i=1}^{M} \langle P(k_u, k_v, \omega), \Phi_i \rangle \Phi_i \qquad (15)$$

with the actual physical array data, that is $P(k_u, k_v, \omega)$.

Then, we calculate a signal to error(noise) ratio via

$$SNR = 10 \log_{10} \frac{|P(*)|^2}{|P(*) - \hat{P}(*)|^2} \, dB.$$

Note that the length of each vector is governed by the number of samples in the aperture, and the number of basis vectors is governed by that of temporal frequencies. The results showed that a linear combination of the orthonormal basis functions can produce a good estimate of the physical array data.

In our experiment, we used 64 samples in aperture $u \in [-256, 256]$ with sample spacing $\Delta_u = 8(meters)$ which satisfies the condition to avoid aliasing[4]. The object area which is centered at the origin is within the disk of radius $X_0 = 64$ m and the distance X_1 is 25600 m. We used 64 temporal frequencies with $1/(4X_0)$ as a sample spacing of the wavenumber centered at 5π $(radians/m)$.

For one point target at the center of target region, i.e., $(x, y) = (X_1, 0)$, the signal to error (noise) ratio of the estimator for the physical array data is as good as 54.18 dB by using M=33 orthonormal basis functions with the length of N=64. Fig. 4a. and Fig. 4b. shows the actual and estimated physical array data for the centered target.

We also estimate the physical array data from synthetic array basis functions for multi-target in the object area positioned at $(X_1, 0), (X_1, 30)$ and $(X_1 + 30, -20)$ m. Fig. 5a. and Fig. 5b. shows actual and estimated physical array data in the k_u domain for a fixed k_v and temporal frequency. The SNR of the estimator is as good as 31.35 (dB) .

From the coverage in Fig. 2 and Fig.3, the coverage at the base band region(corresponds to echo data from the centered target) gives more closer looks. Thus, the result for centered target gives better SNR than that for off-centered targets. And this is why we need more basis functions of SAR data for better estimation when we have many off- centered targets.

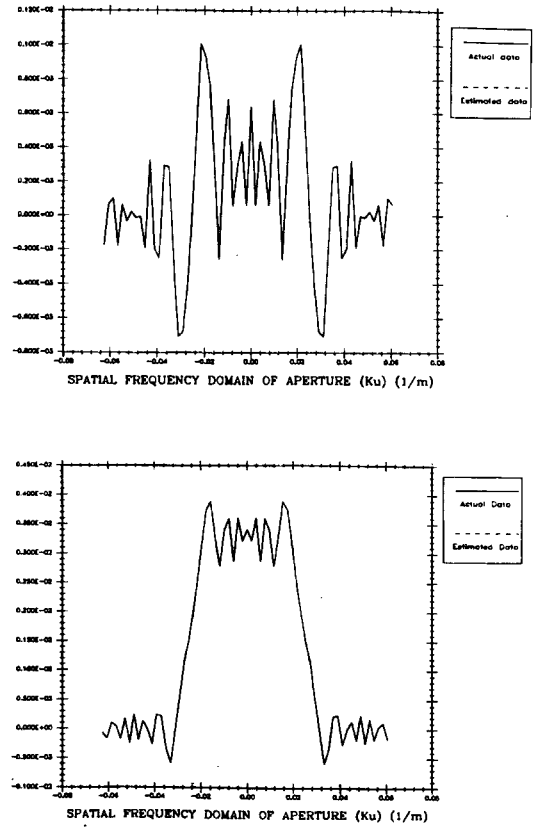

그림 4. 한 개의 centered target을 이용하여 Synthesized array 신호로부터 Physical array 신호 예측, SNR=54.18 dB ; a) 실수 부분, b) 허수 부분

Fig. 4. Estimated physical array data using SAR data basis for one centered target, SNR=54.18 dB; (a) real part and (b) imaginary part.

From all these results, the degree of closeness between two different data sets is different, but still we can conclud that this wavefront inversion

scheme provide a good synthesizing aperture effect.

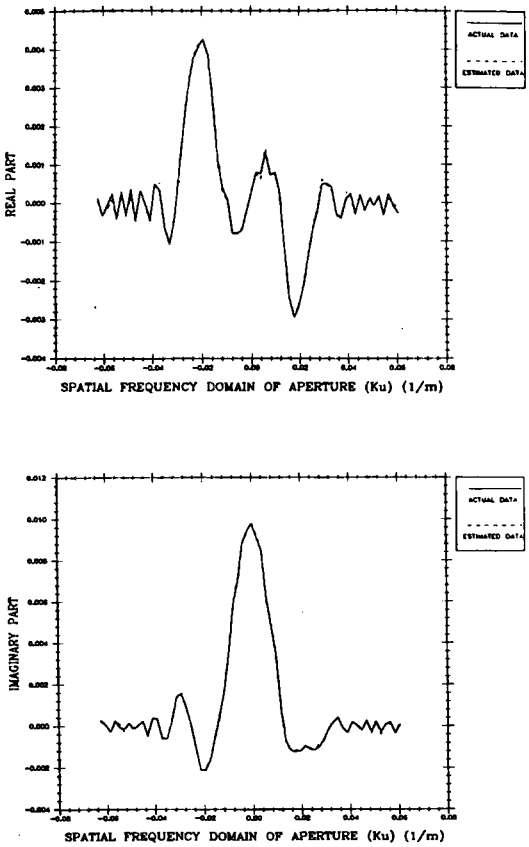

그림 5. 임의의 여러 Targets을 이용하여 Synthesized array 신호로부터 Physical array 신호 예측, SNR=31.35dB ; a) 실수 부분, b) 허수 부분

Fig. 5. Estimated physical array data using SAR data basis for several random targets, SNR=31.35dB; (a) real part and (b) imaginary part.

With the inversion relationship in eq.(6) and eq.(8), we perform the reconstruction with 4 point targets located at $(x, y) = (5, 5)$, $(5, -5)$, $(-5, 5)$, and $(-5, -5)$.

The detailed wavefront reconstruction steps are described in [4]. We simulated the SAR and physical array data with the same system parameters as previous implementation except the target location, and take spatial and temporal Fourier transforms to map the available multidimensional data into the target characteristic function. Then, the two dimensional interpolation was performed with two-dimensional sinc function since the target area is confined within disk of radius X_0.

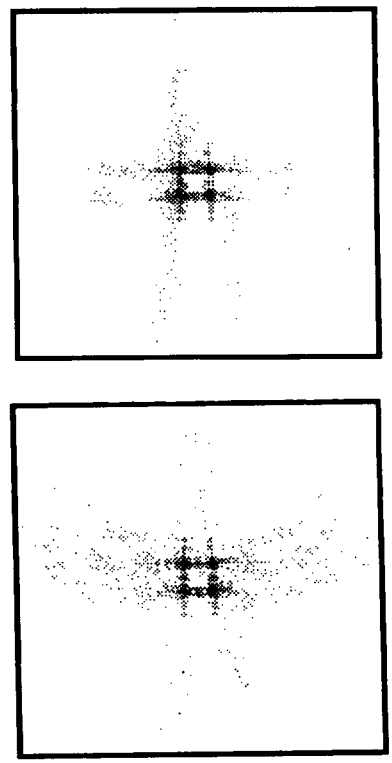

그림 6. Target의 영상복원 ; a) synthesized array data 이용, b) Physical arrary datat 이용

Fig. 6. Reconstructed target image with (a) SAR data and (b) physical array data (contained more artifacts).

The reconstructed image is shown in Fig. 6a, and Fig. 6b from the SAR data and physical array data, respectively. The results with two dimensional SAR data is the same as that with three dimensional physical data. This justify our study for signal subspace comparison. However, even with more data, reconstruction with physical array data gives more numerical errors in implementation because we have to go through two spatial Fourier transforms for u and v domain.

Ⅳ. Conclusion

We introduced an approximation-free inversion scheme -wavefront reconstruction- in SAR imaging and showed the synthesized aperture actually working as an physical antenna of the same size. This was proved by comparing signal subspace of physical and synthesized array data theoretically and numerically. The results showed that the synthesized array data fully span the physical array data with the same system geometry and strongly support the previously proposed inversion scheme valuable in high resolution radar imaging.

References

[1] D. Ausherman, "Developments in radar imaging", *IEEE Trans. Aerospace and Electronic Systems*, 20:363, July 1984.

[2] J. C. Curlander and R. N. McDonough, *Synthetic Aperture Radar*, New York : Wiley, 1991.

[3] M. Soumekh, "Reconnaissance with ultra wideband UHF synthetic aperture radar," *IEEE Signal Processing Magazine*, vol.12, no. 4, pp. 21-40, July 1995.

[4] M. Soumekh, " A system model and inversion for synthetic aperture radar imaging," *IEEE Transactions on Image Processing*, January 1992.

[5] P. Morse and H. Feshbach, *Methods of Theoretical Physics*, New York : McGraw-Hill, 1968.

[6] M. I Skolnik, *Introduction to Radar Systems*, New York: McGraw-Hill, 1980.

저 자 소 개

崔 貞 姬(正會員)

1986년 2월 경북대학교 전자공학과 학사. 1989년 2월 뉴욕주립 버팔로 대학교(SUNY at Buffalo) 전기 및 컴퓨터공학과(Dept. of Electrical and Computer Engineering) 석사. 1992년 6월 뉴욕주립 버팔로 대학교 전기 및 컴퓨터공학과 박사. 1994년 1월 ~ 1998년 2월 SK 텔레콤 중앙연구소 선임연구원, 1998년 3월 ~ 현재 대구대학교 공과대학 정보통신공학부 전임강사. 주관심분야는 Remote Sensing(레이다 Imaging), Inverse Scattering, Wireless Communication